

# Background Simulations for the International Linear Collider

Adrian Vogel\*

2007-11-12

## Abstract

This document gives a brief overview of the ILC machine and detector, beam-related backgrounds, and the simulation tools which can be used to study the impact of these backgrounds on the detector. Simulation results for the vertex detector and the TPC are presented.

## 1 The International Linear Collider

Now that the Large Hadron Collider (LHC) and its detectors are almost fully commissioned and ready to start operation, there is general agreement in the high-energy physics community that the next large-scale project should be an electron-positron collider with a centre-of-mass energy in the TeV range.

The most advanced proposal is the International Linear Collider (ILC), which will use two linear accelerators [1] based on superconducting technology to collide bunches of electrons and positrons. The baseline configuration (about 31 km long) will reach a centre-of-mass energy of  $\sqrt{s} = 500$  GeV, allowing for an upgrade to 1 TeV. The collider will provide a luminosity of  $\mathcal{L} = 2 \cdot 10^{34} \text{ cm}^{-2} \text{ s}^{-1}$  and both beams can be polarised up to a degree of 60% to 80%. The beams will be structured in particle bunches with a separation of 300 ns, 2820 of which will form a so-called bunch train with a length of approximately 1 ms. These bunch trains will be accelerated with a repetition rate of 5 Hz.

The ILC will be a high-precision tool for research at the high-energy frontier, complementary to the proton-proton collider LHC. Physics processes at the ILC will start from a well-defined initial state with precisely known energy and polarisation, and the detector will run in a clean experimental environment with low backgrounds. The LHC will likely discover the Higgs boson and SUSY particles (if they exist in nature), but the ILC will be indispensable to determine their exact properties (e. g. spins or the Higgs self-coupling) and to confirm that the new particles actually behave as predicted by theory [2]. Furthermore, the ILC will be sensitive to small quantum corrections, thereby possibly providing access to energy ranges which would probably be never be reachable by any particle accelerator directly.

---

\*DESY FLC, 22603 Hamburg, Germany, [adrian.vogel@desy.de](mailto:adrian.vogel@desy.de)

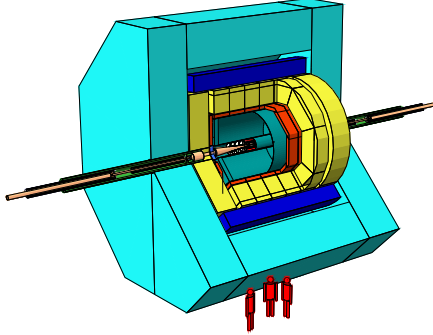


**Figure 1:** Overall view of the LDC detector

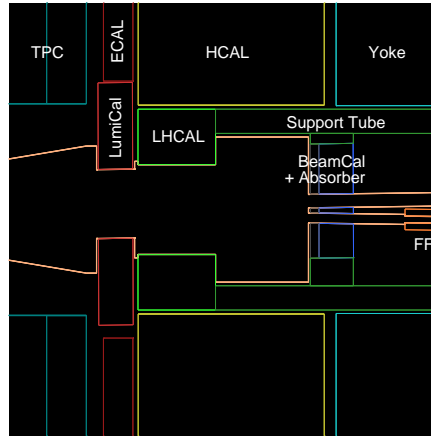


**Figure 2:** Cross section of the LDC forward region (compressed 1:2)

## 2 The Large Detector Concept

The ILC needs detectors [3] with maximum performance: In order to meet the precision goals, a detector has to be able to reconstruct individual particles (also inside jets) and to provide an excellent momentum ( $\delta(1/p_T) < 5 \cdot 10^{-5} \text{ GeV}^{-1}$ ) as well as vertex ( $\delta b \approx 5 \mu\text{m}$ ) resolution.

The so-called Large Detector Concept (LDC, figure 1) [4] is one of four detector concepts which are being developed concurrently in order to find the best possible detector design for the ILC. The LDC features a silicon pixel vertex detector plus further silicon tracking devices close to the interaction point, a gaseous time projection chamber (TPC) as the main tracker, and highly granular calorimeters for both electromagnetic and hadronic particles. The whole detector is enclosed in a solenoidal magnetic field of 4 T, with additional muon chambers in the magnet yoke.

Overall, the LDC is optimised for “Particle Flow”: Since the resolution of the tracking devices is much better than that of the calorimeters up to very high energies, the idea is to reconstruct all charged particles with the help of the tracker, using the calorimeters only for the measurement of neutral particles (photons in the ECAL, neutral hadrons mostly in the HCAL). For isolated particles this is straightforward, but the challenge lies in the decomposition of hadronic jets, especially when they are tightly boosted. Even though particle flow needs a very fine segmentation of the calorimeters and sophisticated reconstruction algorithms, it is currently believed to be the most promising approach to reach an ultimate detector performance.

## 3 Beamstrahlung at the ILC

### 3.1 Production of Photons and Pairs

Since a high luminosity is essential for the measurements, the beams of the ILC have to be focussed to an extremely small spot at the interaction point. The

current set of beam parameters foresees a transverse bunch size of  $\sigma_x = 500$  nm and  $\sigma_y = 5$  nm. To compare, this is 1/1000 of the size of the LEP<sup>1</sup> beams in each dimension.

Due to their small size, the particle bunches have very high electric space charges and are therefore accompanied by strong electric fields. Particles in the oncoming bunch are deflected in a way that the bunch size is reduced further – this is known as the pinch effect and increases the luminosity again, approximately by a factor of two.

As a side effect, photons – the so-called beamstrahlung – can be emitted in the beam-beam interaction [5]. The largest fraction of these photons leaves the detector through the beam tube, only to be absorbed in the beam dump. However, some can also scatter and create electron-positron pairs. These pairs have typical energies of a few GeV and are usually emitted at very small polar angles because of the energy imbalance of the colliding photons. Depending on the beam parameters, around  $10^5$  such particles are created per bunch crossing, resulting in a total energy of around 100 TeV per bunch crossing.

### 3.2 Pairs as a Source of Background

The electron-positron pairs from beamstrahlung scattering are a main source of background for the ILC detector. If the particles have a large polar angle, they can traverse one or more layers of the vertex detector, thereby leaving a charge signal. Even though only a small fraction of the background particles has a high enough transverse momentum, these background hits are actually dominating the occupancy of the vertex detector and are therefore driving the requirements for the readout of the silicon sensors – the electronics for these devices are rather slow and typically pile up the signals of hundreds of bunch crossings.

A large part of the electron-positron pairs hits a low-angle forward calorimeter called BeamCal, covering polar angles of  $5 \text{ mrad} < \theta < 45 \text{ mrad}$ . This device is – among other purposes – designed to detect beamstrahlung pairs and to provide a fast feedback for beam alignment and stabilisation from the spatial distribution of the pairs, which follows a distinct pattern. The BeamCal has to withstand a large radiation dose, and its sensors are specifically designed with radiation hardness in mind, using either special silicon or even diamond sensors in the innermost parts [6].

The electromagnetic showers which are induced in the BeamCal lead to a certain amount of backscattering of secondary electrons, positrons, and photons into the inner parts of the detector. This backscattering can be reduced by a graphite absorber which is mounted in front of the BeamCal, but it cannot be completely avoided. Charged particles at low energies follow the magnetic field lines and are confined to the inner regions of the detector – they are unable to reach the main tracker or the main calorimeters, but they can hit the vertex detector and further contribute to the silicon occupancy. In contrast to that, photons are unaffected by the magnetic field and can also reach the outer sub-detectors, such as the TPC where they can interact through the photoelectric effect or Compton scattering.

---

<sup>1</sup>The Large Electron-Positron Collider (LEP) at CERN was a circular collider with a circumference of 27 km and a maximum centre-of-mass energy of 209 GeV.

Finally, neutrons can be produced in electromagnetic showers by photonuclear reactions. They can travel through the detector almost freely, often reflected from surfaces but sometimes also traversing significant amounts of solid material. Inside the TPC they can scatter with protons (i. e. nuclei of hydrogen which is contained in the quencher gas), thereby producing short recoil tracks. When they are captured in the calorimeters, secondary particles such as photons and neutrons may be emitted in the process.

## 4 Simulation Tools

### 4.1 Guinea-Pig – Pairs Generator

Guinea-Pig [7] is a program which simulates the beam-beam interaction of two colliding particle bunches on a microscopic level. Given a set of beam parameters (centre-of-mass energy  $\sqrt{s}$ , bunch sizes  $\sigma_x$  and  $\sigma_y$ , emittances  $\varepsilon_x$  and  $\varepsilon_y$ , total bunch charge  $Q$ , and others), Guinea-Pig will – among other data – generate the electron-positron pairs which are created in one bunch crossing.

For the studies presented here, the pair-induced backgrounds of 100 bunch crossings were simulated for each of the three beam parameter settings [8] which are commonly known as “ILC Nominal” (the baseline parameter set for the ILC), “ILC Low Power” (a modified parameter set with fewer bunches per train, but a smaller bunch size to recover the luminosity), and “TESLA” (the baseline parameter set for the TESLA accelerator, a predecessor project of the ILC). All simulations were done for  $\sqrt{s} = 500$  GeV.

### 4.2 Mokka – Full Detector Simulation

Mokka [9] is a full simulation for the LDC detector. It is based on the Geant4 framework [10], which is one of the standard tools (not only in high-energy physics) to simulate the interaction of particles with matter. Mokka contains a geometry model of the LDC detector and can take the pairs from Guinea-Pig as its input, firing them into the detector and writing out the hits in the different subdetectors.

A close-up view of the LDC forward region (seen from the top) is shown in figure 2. The interaction point is far on the left, whereas the picture contains the region around  $2\text{ m} < z < 4\text{ m}$ . One can recognise the two major forward calorimeters, the LumiCal ( $100\text{ mm} < r < 350\text{ mm}$ ,  $2270\text{ mm} < z < 2470\text{ mm}$ ) and the BeamCal ( $20\text{ mm} < r < 165\text{ mm}$ ,  $3550\text{ mm} < z < 3750\text{ mm}$ ) with a graphite absorber disk of 50 mm in front [6]. Both calorimeters are not exactly placed on the  $z$ -axis, but centred on the axis of the outgoing beam. The beams collide under a small crossing angle of 14 mrad, and in figure 2 the beam tubes for the incoming and the outgoing beams can be seen on the right. A so-called anti-DID field [11] is superimposed on the main solenoidal field in order to bend the field lines along the path of the outgoing beam, thereby reducing backscattering of particles from the BeamCal.

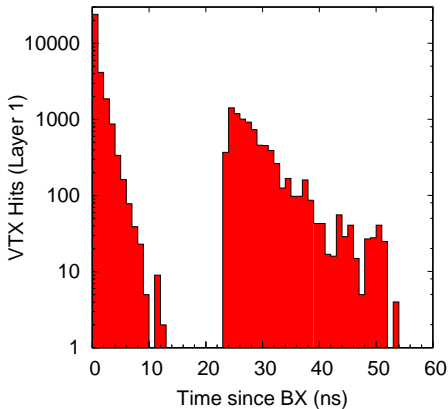


**Figure 3:** Time distribution of hits on the innermost VTX layer

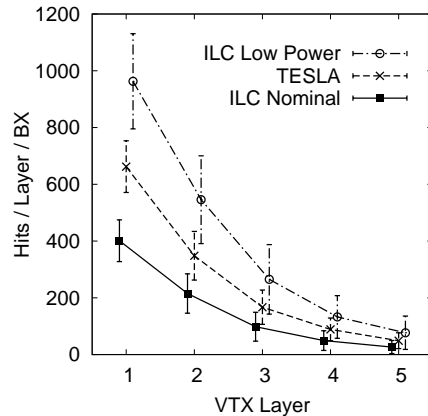


**Figure 4:** Number of hits on the different VTX layers

## 5 Simulation Results – Vertex Detector

### 5.1 Time Structure

Figure 3 shows a histogram of time structure of the vertex detector hits, starting from the moment of the bunch crossing. There is a clear separation between two kinds of hits: Most appear immediately or a very short time (a few nanoseconds) after the bunch crossing – they can only be caused by particles which come directly from the interaction point or which are scattered at a short distance.

After  $t = 23$  ns, a second wave of particles begins to reach the vertex detector. Assuming most of the particles are still highly relativistic and travel nearly at the speed of light, this time interval can be converted to a distance of 7.0 m, which is quite exactly twice the distance of the BeamCal surface from the interaction point. This shows that basically all of the backscatterers which hit the vertex detector come from the BeamCal, and that the BeamCal is the point where backscattering has to be reduced as well as possible.

It should be noted that the time resolution of the silicon sensors will probably not be high enough to resolve the structure from figure 3, therefore it will not be possible to suppress background signals by a simple time cut.

Layer	$r$ (mm)	$\ell$ (mm)	$A$ (cm <sup>2</sup> )	Hits (cm <sup>-2</sup> )
1	15	100	94	$4.26 \pm 0.78$
2	25	250	392	$0.55 \pm 0.18$
3	38	250	597	$0.16 \pm 0.09$
4	49	250	770	$0.06 \pm 0.05$
5	60	250	942	$0.03 \pm 0.02$

**Table 1:** Density of VTX hits per BX for nominal beam parameters

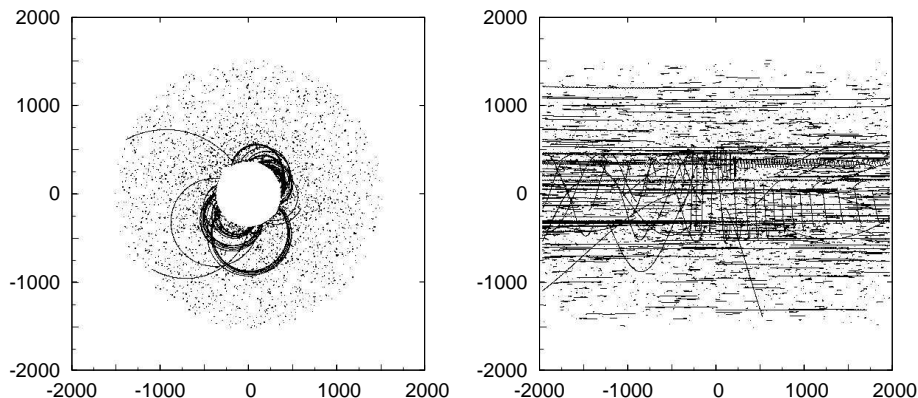


**Figure 5:** Front view (left) and side view (right) of Mokka hits in the TPC from 100 bunch crossings

## 5.2 Total Number of Hits

Figure 4 shows the number of hits per bunch crossing on each of the five vertex detector layers. (The error bars show the standard deviation per bunch crossing, not the total statistical error.) The three curves correspond to the three different beam parameter sets mentioned in section 4.1.

For the nominal beam parameters the numbers range between 400 hits on the innermost layer and 20 hits on the outermost layer. Normalisation with respect to the surface of each layer yields the numbers shown in table 1. The occupancy of the innermost layer is by far the highest, thus driving the technology requirements or maybe even needing a different readout scheme than the rest of the vertex detector.

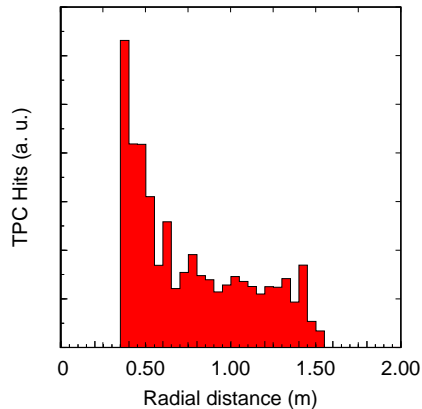
The numbers for the other beam parameter sets are significantly larger. However, the higher backgrounds of the TESLA beam parameters can directly be linked to their higher luminosity ( $3.4 \cdot 10^{34} \text{ cm}^{-2} \text{ s}^{-1}$  instead of  $2.0 \cdot 10^{34} \text{ cm}^{-2} \text{ s}^{-1}$ ). The total number of bunches per bunch train in the “Low Power” setting is almost a factor of two lower than in the nominal setting, meaning the integrated occupancy is not as severe as it may look in figure 4.

# 6 Simulation Results – TPC

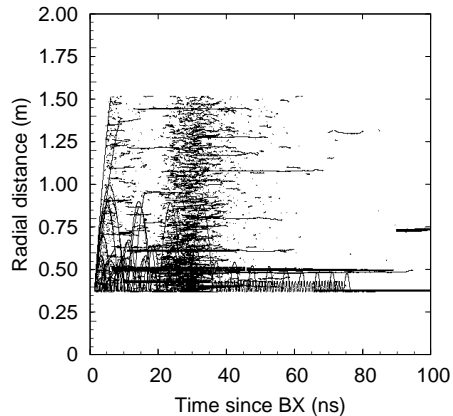
## 6.1 Hit Patterns in the Chamber

Figure 5 shows an image of the hits from 100 bunch crossings in the TPC. Since the drift of electrons through the TPC gas volume takes a relatively long time, the TPC must be considered a rather slow device which accumulates signals from many bunch crossings. Depending on the choice of the chamber gas and the detailed parameters, the TPC of the LDC detector will integrate over 100 to 160 bunch crossings – therefore the picture in figure 5 is more or less realistic, except that it lacks the drift of the charges between the single bunch crossings.

In the front view ( $xy$ -projection), one can clearly see very few high-energy tracks which can actually leave the chamber, a couple of medium-energy curlers which stay close to the inner wall of the chamber, and lots of almost randomly-



**Figure 6:** Radial distribution of hits in the TPC



**Figure 7:** Radius-vs-time distribution of hits in the TPC

distributed dots which do not belong to any track and which are sometimes called “salt and pepper” hits. However, the side view ( $xz$ -projection) shows that most of these hits belong to low-energy particles which curl very tightly, but which nevertheless cover a significant distance (centimetres to metres) through the chamber gas.

These hits can be explained by photons which enter the chamber (leaving no tracks as uncharged particles) and release an electron from the chamber gas at some point in space through the photoelectric effect or Compton scattering. The energy of these particles is high enough to leave a sizable track, at least in the  $z$ -direction.

## 6.2 Distribution of the Hits

Figure 6 shows the radial distribution of the TPC hits. The occupancy is significantly higher in the inner regions of the chamber than in the rest of the detector volume. It should be noted that figure 6 is not corrected for the increasing volume of the cylinders which correspond to the histogram bins, therefore an approximately constant height of the histogram bins means a  $1/r$  decrease of the number of hits per unit of volume.

It can clearly be seen that the simulation of 100 bunch crossings – even though it may take roughly half a CPU-year on a Pentium-4-like processor – is not sufficient to cancel out statistical fluctuations completely. These fluctuations are very large, since already a single medium-energy curler can create an enormous number of hits in the chamber, depending on its longitudinal momentum.

The visualisation in figure 7 is rather uncommon, but it provides some information which can usually not be seen: Similar to figure 3, it shows the time distribution of hits in the TPC, starting from the moment of the bunch crossing. The second coordinate contains the radial position of the hits, measured from the  $z$ -axis.

In the left part of the plot, most hits obviously belong to tracks which come from the interaction point and which either leave the TPC or curl through

the chamber more or less tightly. Only few low-energy tracks are caused by photons. After slightly more than 20 ns, a large number of low-energy tracks appears throughout the whole chamber, with a very high density close to the inner wall. Like in figure 3, these signals are caused by photons which are backscattered from the surface of the BeamCal.

What can be seen in figure 7 as well is the fact that there are also a few hits which appear a long time after the bunch crossing, with delays in the order of microseconds up to milliseconds. These hits are caused by photons which come from decaying nuclei, which were in turn excited by neutron capture or other nuclear reactions.

## 7 Summary and Outlook

Electron-positron pairs created by the scattering of beamstrahlung photons are a main source of background at the ILC. Their production has to be kept in mind when choosing a set of beam parameters for the machine. Hits by pair particles which come directly from the interaction point cannot be avoided, but a significant contribution is due to backscattering from the forward region. Therefore, the forward region (and the magnetic field configuration) of the detector has to be designed carefully, with the suppression of backscattering as one of the optimisation goals.

Pair backgrounds have an important impact on the design of the vertex detector – the expected background occupancy and also the integrated radiation dose might well influence the decision for one of the many technology options which are currently being studied for the vertex detector [12].

In contrast to that, the impact of the backgrounds on the TPC currently gives no reason for concern. Hit patterns as shown in figure 5 can easily be detected and eliminated by pattern recognition algorithms during the data reconstruction, and the single readout units of the TPC (so-called voxels) are so small that the final background occupancy is almost negligible, except maybe in the innermost parts of the chamber.

Even though the direct effects of the backgrounds seem to be no problem, it still has to be checked whether the electric field inside the chamber will be distorted by the additional charges which are created by background hits. Slowly-drifting ions might build up space charges which are high enough to influence the drift of electrons through the chamber and which might deteriorate the resolution, but this will have to be checked with detailed studies.

Finally, a full test run of the whole software chain [13] – simulation of physics events and backgrounds with large statistics, digitisation, pile-up, track finding, track fitting, and analysis – is needed to provide a realistic estimate of the impact of backgrounds on the physics performance of the detector. For this purpose, the whole software chain is currently being refined, and simulation runs with large statistics (e. g. a whole bunch train with 2820 bunch crossings) are foreseen.



## References

- [1] N. Phinney, N. Toge, N. Walker (eds.),  
ILC-Report-2007-001, Part 3 – Accelerator (2007).
- [2] A. Djouadi, J. Lykken, K. Mönig, Y. Okada, M. Oreglia, S. Yamashita  
(eds.), ILC-Report-2007-001, Part 2 – Physics (2007).
- [3] T. Behnke, C. Damerell, J. Jaros, A. Miyamoto (eds.),  
ILC-Report-2007-001, Part 4 – Detectors (2007).
- [4] D. Kisielewska et al., Detector Outline Document for the Large Detector  
Concept (2006), [www.ilcldc.org/documents/dod/](http://www.ilcldc.org/documents/dod/)
- [5] K. Yokoya, KEK Report 85-9 (1985).
- [6] FCAL Collaboration, [www-zeuthen.desy.de/ILC/fcal/](http://www-zeuthen.desy.de/ILC/fcal/)
- [7] D. Schulte, DESY Report TESLA 97-08 (1997).
- [8] ILC@SLAC Beam Parameters Web Site, [www-project.slac.stanford.edu/ilc/acceldev/beamparameters.html](http://www-project.slac.stanford.edu/ilc/acceldev/beamparameters.html)
- [9] Mokka Web Site, [mokka.in2p3.fr](http://mokka.in2p3.fr)
- [10] S. Agostinelli et al., NIM A 506 (2003) 250–303.
- [11] B. Parker and A. Seryi, Phys. Rev. ST Accel. Beams 8, 041001 (2005).
- [12] ALCPG 2007 Vertex Detector Review, [ilcagenda.linearcollider.org/conferenceDisplay.py?confId=2208](http://ilcagenda.linearcollider.org/conferenceDisplay.py?confId=2208)
- [13] ILCSOFT Web Site, [ilcsoft.desy.de](http://ilcsoft.desy.de)